Ultrafast Short-Range Disordering of Femtosecond-Laser-Heated Warm Dense Aluminum

P. M. Leguay,[1] A. Lévy,[2] B. Chimier,[1] F. Deneuville,[1] D. Descamps,[1] C. Fourment,[1] C. Goyon,[1] S. Hulin,[1] S. Petit,[1] O. Peyrusse,[1] J. J. Santos,[1] P. Combis,[3] B. Holst,[3] V. Recoules,[3] P. Renaudin,[3] L. Videau,[3] and F. Dorchies[1,*]

[1]*Université Bordeaux, CNRS, CEA, CELIA (Centre Lasers Intenses et Applications), UMR 5107, F-33400 Talence, France*

[2]*Ecole Polytechnique, LULI (Laboratoire d'Utilisation des Lasers Intenses), UMR 7605, F-91128 Palaiseau, France*

[3]*CEA-DAM-DIF, F-91297 Arpajon, France*

(Received 18 July 2013; published 11 December 2013)

We have probed, with time-resolved x-ray absorption near-edge spectroscopy (XANES), a femtosecond-laser-heated aluminum foil with fluences up to 1 J/cm^2. The spectra reveal a loss of the short-range order in a few picoseconds. This time scale is compared with the electron-ion equilibration time, calculated with a two-temperature model. Hydrodynamic simulations shed light on complex features that affect the foil dynamics, including progressive density change from solid to liquid ($\sim$ 10 ps). In this density range, quantum molecular dynamics simulations indicate that XANES is a relevant probe of the ionic temperature.

DOI: 10.1103/PhysRevLett.111.245004 PACS numbers: 52.50.Jm, 52.27.Gr, 52.38.Mf, 61.05.cj

The current advance in femtosecond lasers allows us to bring and study the matter in extreme states, such as warm dense matter, and to achieve strong thermal disequilibrium between electrons and ions. Studying the way strongly excited and out-of-equilibrium matter relaxes enables us to understand the electron-ion equilibration and to evaluate the time scale of this process.

Focused on a metal, an optical femtosecond laser mainly excites the electrons that oscillate in the laser field. The energy is absorbed within the pulse duration. The equilibration with the lattice occurs on a longer time scale. Below and near the damage threshold, this process has already been investigated theoretically [1] and with optical reflectivity experiments (Refs. [2–4] and references therein). At these moderate excitation levels, the energy transfer to the lattice is driven by electron-phonon coupling independent of the electron temperature. At higher excitation levels, the electron-ion coupling becomes more complex. The influence of electron temperature is predicted to become significant, strongly depending on the material under consideration [5]. Phase transitions may occur on the equilibration time scale, so that the material hydrodynamics should be considered. Furthermore, a theoretical paper indicates that, in some transition metals, the electronic density of states, then the lattice cohesion, may be affected by high electron temperature in large off-equilibrium situations [6]. This may induce modification of phase transition dynamics, as reported in a recent experiment that suggests electronic bond hardening in warm dense gold [7].

The dynamic interplay between electron and ion structures basically occurs at the atomic scale. Well above the damage threshold, the energy transfer from electrons to the lattice leads first to long-range order breaking, then to progressive short-range disordering. In order to investigate this dynamics, several approaches have been endeavored. Time-resolved optical reflectivity measurements have been used to follow the solid-to-liquid transition phase in aluminum [3]. This diagnostic is relatively easy to implement. But, as the relationship between optical properties and electron structure depends on models, it only gives indirect measurements. Recent techniques of time-resolved x-ray [8,9] and electron [7,10] diffraction provide direct access to the lattice structure at the atomic scale. As diffraction intrinsically relies on the long-range order, it gives information below or near the melting. Time-resolved x-ray absorption near-edge spectroscopy (XANES) [11] has been exploited in a recent study performed by Cho *et al.* [12] to investigate the electronic temperature evolution. But, it could also be particularly suited to probe the short-range order dynamics in warm dense matter situations well beyond the melting.

In this Letter, we present a new experimental approach to study the electron-ion equilibration dynamics in a femtosecond-laser-heated warm dense material. We perform time-resolved XANES measurements on aluminum foils heated with fluences up to 1 J/cm^2. They reveal the picosecond dynamics of the short-range disordering. Results are interpreted as the increase of ion temperature up to equilibration, with simulations including the two-temperature model (TTM) [13] and a careful hydrodynamical description. This study is supported by *ab initio* quantum molecular dynamics (QMD) simulations, establishing that XANES is still a relevant diagnostic of ion temperature in this regime, even if the density goes from the solid down to the liquid one.

As features well established in XANES analysis, the spectral range up to $\sim$10 eV above the K edge is affected by the electron structure, while the oscillatory structures that follow reveal the short-range order [11]. Previous studies have been performed on warm dense aluminum XANES spectra [14–16] at thermal equilibrium. They have demonstrated that the amplitude of such XANES modulations

decreased with the temperature and disappeared above ~0.5 eV. As the short-range order is related to the ion spatial distribution, the ion temperature is intrinsically diagnosed in out-of-equilibrium situations, rather than the electron temperature. In addition to these considerations, we have chosen to study warm dense aluminum for another reason. Aluminum is a simple metal whose electron structure is very close to Fermi electron gas. As a consequence, the electron-phonon coupling factor is not supposed to strongly depend on electron temperature [5]. Furthermore, no electronic bond hardening is expected [6].

This experiment has been carried out on the Eclipse laser facility at CELIA. A 100 nm aluminum foil is heated by a p-polarized laser pulse at 800 nm central wavelength, with 120 fs duration FWHM. The angle of incidence is set at 60°. The full setup is detailed in Ref. [17]. The Al sample is probed by a broadband laser-plasma x-ray source, optimized near the K edge (1.559 keV) [18]. Its duration is 3.15 ± 0.25 ps rms. The absorption spectra are measured by using a double crystal spectrometer [19]. The delay between the laser pump and the x-ray probe pulses is scanned in order to get time resolution. The heating incident fluence is controlled by the laser pulse energy. In order to estimate the deposited energy in the sample, the laser absorption level is deduced from reflectometry measurements.

Figure 1 (left) exhibits some XANES spectra recorded for an incident laser fluence of 0.27 ± 0.05 J/cm^2. The corresponding measured laser absorption is $25\% \pm 4\%$. Each spectrum is the result of cumulation over ~30 shots. The residual noise mainly comes from photon counting statistics on the detector. The first XANES spectrum (delay $= -2.5$ ps) is similar to a "cold" spectrum, measured without heating and with higher statistics. Comparison between them allows us to evaluate the noise level. The modulations that follow the K edge reveal the high level of short-range order of the face-centered-cubic atomic structure of solid state aluminum. After heating, their amplitude decreases but some modulations significantly remain at long delay (82.5 ps), as can be seen when comparing with a "warm" spectrum measured at higher fluence. No preedge structure is observed, indicating that the density remains close to the solid one [17,20], up to ~100 ps (limit of measurements). As demonstrated in previous studies [20,21], the first bump after the K edge could be affected by the electronic structure modifications with temperature or density. That is why we consider the second bump, far enough from the K edge (~ 30 eV), to retrieve the short-range order level.

The amplitude of the second bump is estimated from the integral of the spectrum from 1.59 to 1.61 keV, above the warm spectrum shown in Fig. 1 (left). Figure 1 (right) summarizes the time evolution of this amplitude for several laser fluences. The instrumental response is displayed in the figure, i.e., the convolution of an instantaneous and complete loss of XANES modulations with the finite duration of the x-ray probe (3.15 ± 0.25 ps rms). At very high fluence (data extracted from Ref. [17] at 6 J/cm^2), the measurements fit with the instrumental response. In such a situation, the short-range order is decreased in a very short time scale compared to time resolution, and so strongly that XANES modulations can no longer be observed, even if the matter is not yet completely equilibrated. In that sense, one should consider XANES modulations as a "saturated" diagnostic of the short-range disordering. At 0.8 J/cm^2, the same behavior is observed. At 0.27 J/cm^2, since XANES modulations still remain at long delay, their temporal evolution reflects the full short-range order dynamics ("unsaturated" diagnostic). It significantly differs

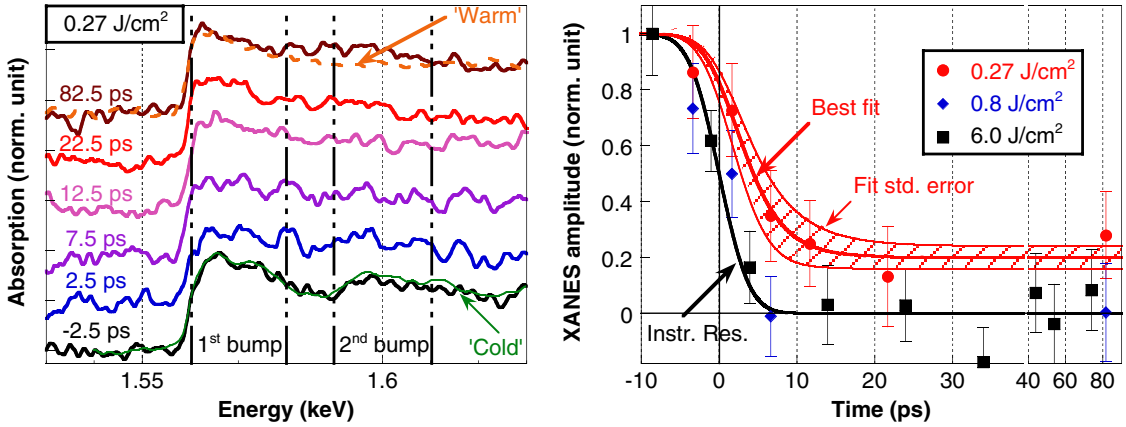

FIG. 1 (color online). Left: normalized XANES spectra of a 100 nm aluminum foil irradiated by a 120 fs laser pulse at 0.27 ± 0.05 J/cm^2, measured as a function of time delay between the laser pump and the x-ray probe. A warm spectrum is presented with ion temperature estimated at 1 eV. A reference cold spectrum is reported for comparison. Spectra are vertically shifted for clarity reasons. Right: time evolution of the XANES second bump amplitude, for several laser fluences (the 6 J/cm^2 data are extracted from Ref. [17]). The estimated instrumental response is reported for comparison. The 0.27 J/cm^2 data are fitted with a simple model giving the characteristic time of the short-range disordering.

from the instrumental response. In order to retrieve a characteristic time, we apply the following procedure. We first consider that ion temperature can be described by $T_i = T_{\mathrm{fin}}[1 - \exp(-t/\tau_{\mathrm{eq}})]$, as a classical result from the TTM, τ_{eq} being the characteristic equilibration time and T_{fin} the temperature achieved at equilibration. Second, we assume that the XANES amplitude is a linear function of T_i as far as it can be observed (estimated from Ref. [16]). Error bars are, however, too high in this previous study to retrieve an accurate absolute value of T_{fin} (beyond the scope of the Letter). The best fit gives $\tau_{\mathrm{eq}} = 3.5 \pm 1.4$ ps. The uncertainty takes into account the noise level on XANES spectra, as well as the pump-probe synchronization accuracy (optically measured).

The electron-ion thermal equilibration can be described by the Anisimov TTM [13]. Its dimensionless version, commonly used to analyze experiments [1,10,12], is reported in the following equations. T_e and T_i are, respectively, the electron and ion temperatures. C_e and C_i are the electron and ion heat capacities, and γ is the electron-phonon coupling factor. They are taken from Lin *et al.* [5]. $S(t)$ describes the absorbed laser energy that is supposed to be deposited on electrons,

$$C_e(T_e)\frac{dT_e}{dt} = \gamma(T_e)(T_i - T_e) + S(t),$$
$$C_i\frac{dT_i}{dt} = \gamma(T_e)(T_e - T_i).$$

At 0.27 J/cm^2 incident fluence, and considering the measured laser absorption level, these equations lead to equilibrated temperature $T_{\mathrm{fin}} = 2750$ K and to equilibration time $\tau_{\mathrm{eq}} = 1.35$ ps that is shorter than measurements. As the foil hydrodynamics can no more be ignored in such a high energy density regime, we performed simulations integrating TTM equations in the one-dimensional hydrodynamic code ESTHER detailed in Ref. [22]. The laser absorption is calculated by solving the Helmholtz equations. The matter evolution is described by hydrodynamics coupled to a two-temperature multiphase equation of state [23], with consistent ion heat capacity. The electron heat conduction is taken from Ref. [24]. Figure 2 summarizes the temporal evolution of the ion temperature and density in a 100 nm aluminum foil heated in the same conditions than the experiment at 0.27 J/cm^2. The calculated level of the laser energy absorption is 25%, consistent with measurements. The ion temperature is homogenized up to the rear side within ~1.5 ps. At this time, a residual excess of temperature remains on the laser side, smaller than 30%. The pressure achieved drives a relaxation of the matter from solid to liquid density (i.e., from 2.7 down to ~2.35 g/cm^3). It starts from the edges and propagates through the foil at the sound velocity (~6 nm/ps). As a consequence of mass conservation, both the front (laser) and rear side surfaces expand at a constant velocity ~1 nm/ps. Note that this value is in close agreement

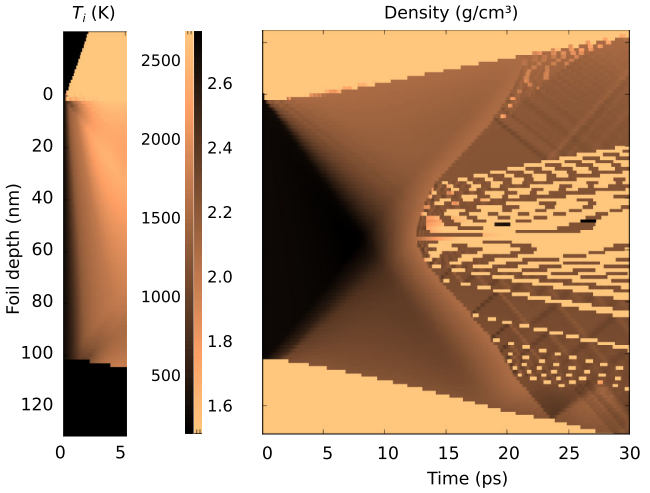

FIG. 2 (color online). Temporal and spatial evolution of ion temperature (left) and density (right), from hydrodynamical code, considering the same conditions as the experiment at 0.27 J/cm^2. The incident laser comes from the top.

with recent optical measurements performed with similar absorbed fluence [25]. Once the two solid-liquid density interfaces intersect, the foil is separated into two liquid slices flowing away from each other. Indeed, the deposited energy is not high enough to vaporize the foil, in agreement with the nonobservation of preedge structure in the XANES spectra recorded at long delay.

When averaging over the foil thickness, the ion temperature temporal behavior is well described by $T_i = T_{\mathrm{fin}}[1 - \exp(-t/\tau_{\mathrm{eq}})]$. Compared to dimensionless TTM, the equilibrated temperature T_{fin} is lowered down to 2050 K, considering that about 25% of the absorbed energy is consumed in kinetic energy (relaxation). The estimated equilibration time $\tau_{\mathrm{eq}} = 1.0$ ps is a bit shorter. In order to determine the possible influence of the thermal conduction, we performed similar hydrodynamic simulations with heat conduction lowered by 1 order of magnitude, then with uniform energy deposit (infinite conduction). Obviously, when the conduction is lowered, the symmetry is affected between the front and rear surfaces. But, τ_{eq} is not significantly changed, once it has been averaged over the foil thickness (i.e., to get data that can be compared with XANES spectra).

Hydrodynamic simulations reveal features that question the validity of XANES modulations as a reliable diagnostic of the short-range order, then T_i, in the conditions explored. Indeed, the density turns from solid to liquid, while the XANES modulation behavior with T_i has been only studied at solid density [16]. In order to remove this ambiguity, we have performed QMD simulations. They calculate ion spatial distributions as well as x-ray absorption spectra, at different temperatures and densities, considering the same general parameters as in Ref. [15]. Results are plotted in Fig. 3. The spatial ion distribution is

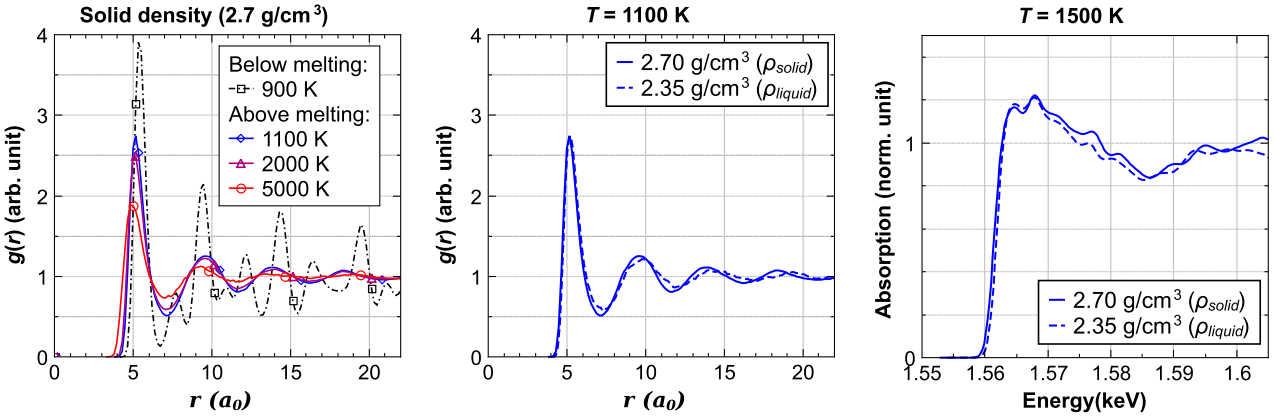

FIG. 3 (color online). QMD calculations performed at electron-ion thermal equilibrium. Left: aluminum ion-ion radial distribution function $g(r)$ for various temperatures at solid density. The distance r between ions is expressed in units of the Bohr radius a_0. Center: $g(r)$ at 1050 K at solid versus liquid densities. Right: XANES spectra at 1500 K at solid versus liquid densities.

represented by the ion-ion radial distribution function $g(r)$ that gives the probability to find neighboring ions as a function of the distance. Below the melting temperature (933 K), this function presents well defined peaks, even at long distance, reflecting the long-range order expected in the solid crystalline phase. Above melting, only the first peaks remain, indicating that the long-range order is lost, but the short-range order is still significant. This short-range order progressively decreases as the temperature increases. Two $g(r)$ are plotted at the same temperature (1100 K) but at solid versus liquid densities. They are very close. The positions of the most distant peaks are a bit shifted, but the first one is unchanged ($\sim 5a_0$). That reveals the interatomic distance is unaffected by the solid-to-liquid density decrease, which results from different compactness between these two phases. As a consequence, the XANES spectrum is not significantly modified, as can be seen in Fig. 3 (right), reporting simulations performed at 1500 K. The same conclusions are observed from real-space finite-difference XANES calculations [26]: (i) XANES modulation amplitudes are not affected by the solid-to-liquid density transition and (ii) they only depend on the short-range order that decreases with ion temperature.

Two reasons could contribute to understand the discrepancy between the measured short-range disordering time ($\tau_{\mathrm{eq}} = 3.5 \pm 1.4$ ps) and the calculated equilibration time ($\tau_{\mathrm{eq}} = 1.0$ ps). The first one comes from the analysis. The assumption that the XANES modulation amplitude decreases linearly with the ion temperature (up to complete XANES vanishing) could be too strong, eventually resulting in an overestimation of τ_{eq}. The second one concerns the physical coefficients commonly used in the TTM [5] and that drive the electron-ion equilibration time: C_e, C_i, and γ. Ion heat capacity C_i is estimated from the Bushman-Lomonosov-Fortov (BLF) equation of state, built from experimental data in a wide range of density-temperature conditions [23]. The electron heat capacity C_e is calculated from the solid state electron density of states (DOS), but takes into account the Fermi-Dirac distribution function that depends on the electron temperature. Previous studies on aluminum have confirmed that the electron DOS remained very close to the Fermi electron gas, even well above the melting temperature (up to a few eV) [27]. Therefore, such an estimation for C_e may be justified. Nevertheless, γ is estimated from electron and phonon DOS, the latter being deduced from the cold solid phase. This assumption is valid below the melting temperature, but it should no longer be correct when the lattice is severely affected above the melting temperature. One should then consider more complex models from dense plasma physics to estimate properly the electron-ion coupling parameter or alternatively the electron-ion collision frequency (Ref. [28] and references therein). A recent paper reporting time-resolved optical measurements on gold reaches the same conclusion [29]. A lower value of γ should be considered that could fit with the slower equilibration observed in this experiment.

In summary, we have explored the potential of a new experimental approach in which time-resolved XANES is used to estimate short-range disordering, as well as electron-ion equilibration. We present XANES spectra of a femtosecond-laser-heated warm dense aluminum foil (up to 1 J/cm^2). They reveal the picosecond dynamics of the short-range disordering. At 0.27 J/cm^2, it occurs within a characteristic time of 3.5 ± 1.4 ps. This time scale is comparable but a bit longer than electron-ion equilibration time deduced from the two-temperature model (1.0 ps in the same situation). Hydrodynamical simulations shed light on a complex heated foil dynamics. As a main feature, the density progressively turns from solid to liquid (~ 10 ps). QMD simulations, as well as real-space finite-difference XANES calculations, attest that the short-range order is preserved during this solid-to-liquid density transition and that XANES is still a relevant diagnostic of the ion

temperature above melting. In this warm dense regime, the electron-ion coupling should be estimated using models more complex than considering the solid phase phonon DOS. That could contribute to explain the longer equilibration time suggested by experimental data.

This work was supported by the French Agence Nationale de la Recherche, under Grant No. OEDYP (ANR-09-BLAN-0206-01) and the Conseil Régional d'Aquitaine, under Grants No. POLUX (2010-13-04-002) and No. COLA2 (2.1.3. 09010502). The authors gratefully acknowledge Rodrigue Bouillaud and Laurent Merzeau for their technical assistance as well as Capucine Medina for her valuable help on the laser.

*dorchies@celia.u-bordeaux1.fr

[1] B. Rethfeld, A. Kaiser, M. Vicanek, and G. Simon, Phys. Rev. B **65**, 214303 (2002).
[2] J. L. HostetlerA. N. Smith, D. M. Czajkowsky, and P. M. Norris, Appl. Opt. **38**, 3614 (1999).
[3] M. Kandyla, T. Shih, and E. Mazur, Phys. Rev. B **75**, 214107 (2007).
[4] E. G. Gamaly, Phys. Rep. **508**, 91 (2011).
[5] Z. Lin, L. V. Zhigilei, and V. Celli, Phys. Rev. B **77**, 075133 (2008).
[6] V. Recoules, J. Clerouin, G. Zerah, P. M. Anglade, and S. Mazevet, Phys. Rev. Lett. **96**, 055503 (2006).
[7] R. Ernstorfer, M. Harb, C. T. Hebeisen, G. Sciaini, T. Dartigalongue, and R. J. D. Miller, Science **323**, 1033 (2009).
[8] A. Rousse *et al.*, Nature (London) **410**, 65 (2001).
[9] K. Sokolowski-Tinten *et al.*, Nature (London) **422**, 287 (2003).
[10] B. J. Siwick, J. R. Dwyer, R. E. Jordan, and R. J. D. Miller, Science **302**, 1382 (2003).
[11] C. Bressler and M. Chergui, Chem. Rev. **104**, 1781 (2004).
[12] B. I. Cho *et al.*, Phys. Rev. Lett. **106**, 167601 (2011).
[13] S. I. Anisimov, B. Kapeliovitch, and T. Perel'man, Zh. Eksp. Teor. Fiz. **66**, 776 (1974) [Sov. Phys. JETP **39**, 375 (1974)].
[14] O. Peyrusse, J. Phys. Condens. Matter **20**, 195211 (2008).
[15] V. Recoules and S. Mazevet, Phys. Rev. B **80**, 064110 (2009).
[16] A. Mancic *et al.*, Phys. Rev. Lett. **104**, 035002 (2010).
[17] F. Dorchies *et al.*, Phys. Rev. Lett. **107**, 245006 (2011).
[18] M. Harmand, F. Dorchies, O. Peyrusse, D. Descamps, C. Fourment, S. Hulin, S. Petit, and J. J. Santos, Phys. Plasmas **16**, 063301 (2009).
[19] A. Lévy, F. Dorchies, C. Fourment, M. Harmand, S. Hulin, J. J. Santos, D. Descamps, S. Petit, and R. Bouillaud, Rev. Sci. Instrum. **81**, 063107 (2010).
[20] A. Lévy *et al.*, Phys. Rev. Lett. **108**, 055002 (2012).
[21] A. Benuzzi-Mounaix *et al.*, Phys. Rev. Lett. **107**, 165006 (2011).
[22] J. P. Colombier, P. Combis, F. Bonneau, R. Le Harzic, and E. Audouard, Phys. Rev. B **71**, 165406 (2005).
[23] A. V. Bushman, I. V. Lomonosov, and V. E. Fortov, Sov. Tech. Rev. B Therm. Phys. **5**, 1 (1993).
[24] B. Chimier, V. T. Tikhonchuk, and L. Hallo, Phys. Rev. B **75**, 195124 (2007).
[25] F. Deneuville, B. Chimier, D. Descamps, F. Dorchies, S. Hulin, S. Petit, O. Peyrusse, J. J. Santos, and C. Fourment, Appl. Phys. Lett. **102**, 194104 (2013).
[26] O. Peyrusse, High Energy Density Phys. **6**, 357 (2010).
[27] A. Lévy *et al.*, Plasma Phys. Controlled Fusion **51**, 124021 (2009).
[28] J. Vorberger and D. O. Gericke, AIP Conf. Proc. **1464**, 572 (2012).
[29] Z. Chen, B. Holst, S. E. Kirkwood, V. Sametoglu, M. Reid, Y. Y. Tsui, V. Recoules, and A. Ng, Phys. Rev. Lett. **110**, 135001 (2013).